A Slim Horizontally Polarized Omnidirectional Antenna Based on Turnstile Slot Dipole

Cheng-Yuan Chin* and Christina F. Jou

Abstract—A novel horizontally polarized (HP) antenna with omnidirectional pattern is presented in this paper. The proposed antenna applies the concept of rotating electric field method to conventional slot dipoles. Two CPW-fed slot dipoles are placed in a perpendicularly conjugate form. By properly arranging the magnitude and phase of input signals, the omnidirectional pattern can be synthesized at broadside. A prototype is developed at the 2.6 GHz band, which offers a horizontally polarized omnidirectional radiation pattern with gain of 2.5–3.4 dBi, and the measured antenna efficiency is greater than 73% through the operating band (2.4–2.8 GHz). Furthermore, a 20-dB polarization purity is achieved in this design. The overall volume of the proposed antenna is $22 \times 22 \times 90 \, \text{mm}^3$ ($0.19\lambda_0 \times 0.19\lambda_0 \times 0.78\lambda_0$). Distinct from the other proposed HP antennas provided with planar geometry, this antenna is slim in shape, and it can be readily integrated with vertical dipoles to form a polarization diversity system in current wireless router and AP applications.

1. INTRODUCTION

In wireless communication systems, antennas with omnidirectional radiation pattern can ensure full coverage and are widely adopted for indoor and base station applications. Most existing systems are vertically polarized, and these antennas can be simply realized by vertical dipoles. But the polarization of propagating electromagnetic wave will change significantly due to the complicated surrounding environment. Recently, the requirement of horizontally polarized omnidirectional antennas has increased rapidly as they can serve as the diversity counterparts for vertically polarized ones.

For a 3G network, the dual-polarized antenna, which is the combination of orthogonally polarized radiators, is often employed to form a multiple-input-multiple-output (MIMO) antenna system that provides polarization diversity. It can transmit or receive wireless signals at both polarizations in all directions of the azimuth plane, and this system has the benefit to harvest the polarization resource [1]. Particularly, the dual-polarized MIMO system can improve the communication performance in increasing the channel capacity and the diversity gain, and mitigating the polarization mismatch between transmitter and receiver. In contrast with the traditional 1×2 (or 2×1) spatial diversity system that separates two single-polarized antenna elements some distance apart, the polarization diversity system saves the space between them and thus reduces the total dimension of the antennas.

According to the antenna theory, the small loop antenna with a uniform current distribution can be considered as a magnetic dipole, which radiates an omnidirectional pattern with horizontal polarization. However, it has very small radiation resistance and high reactance [2], causing difficult impedance matching. For this reason, the most common approach is to produce a horizontally annular current distribution instead of the small loop.

Alford loop antenna is a classical design among horizontally polarized omnidirectional antennas [3–5]. It can be regarded as the combination of two dipoles, and two arms of each dipole form a right angle. However, this design suffers from narrow bandwidth (less than 10%) owing to difficulties in impedance matching. So far, several antenna designs with increased operational bandwidth have been reported.

The first wideband configuration was attributed to the work by Wu and Luk [6]. They developed a circular array consisting of four magneto-electric dipoles to form an HP omnidirectional radiation pattern. Although this antenna has an impedance bandwidth of 38%, it is a 3D structure made of metal, which occupies larger area than planar PCB antennas. In [7], four curved printed dipoles with parasitic strips can achieve a 30% bandwidth, which can operate over WLAN band of 5.1–6.8 GHz. Later, Quan et al. had improved this prototype employing a broadband balun, and removed the parasitic elements for size reduction. It has a bandwidth of 31% for 2G/3G base-station applications [8]. Instead of using dipole radiators, Wei et al. proposed a periodically capacitively-loaded loop antenna having a bandwidth of 31.2% [9]. Recently, a wideband HP antenna exhibiting 41% bandwidth has been proposed, which can meet the requirement of 4G Long Term Evolution (LTE) [10].

Another group of horizontally polarized antennas are based on the rotating field technique. Two inputs of conventional crossed dipoles are fed in phase quadrature [11, 12]. These so-called turnstile or superturnstile antennas have been extensively used in TV broadcasting systems. Note that the main beam occurs in the axial direction of the crossed dipole when only one turnstile component is used. Therefore, the commercial turnstile antenna is composed of axially aligned multiples to ensure the azimuth plane has the maximum radiation field.

Slot antennas have an essential advantage over the above-mentioned designs in the applications for volume-limited systems. They can be easily disguised as poles or masts in urban area. In [13–15], several HP omnidirectional slot antennas were proposed. A substantial problem was pointed out that the deviation of radiation pattern would be negligible only in a narrow bandwidth [15]. The reason is that there is just one longitudinal slot in the azimuth direction. To obtain a smooth radiation pattern in a wide frequency range, the slots should be arranged with rotational symmetry [16].

In this paper we present a novel turnstile slot antenna, which replaces the crossed dipole element with a pair of slots in the turnstile antenna configuration. It is more compact than traditional turnstile antenna, especially in the dimension on the azimuth plane. Implementation of the rotating electric field method is verified to synthesize an omnidirectional pattern. Detailed considerations of the proposed design and the experimental results of the fabricated prototype are carefully investigated.

2. OPERATION PRINCIPLE

The rotating electric field method is employed in this paper to achieve an omnidirectional pattern with horizontal polarization in the azimuth plane. First we consider an aperture which is mounted on an infinite ground plane, as shown in Fig. 1(a). Assuming that the tangential component of electric field over the aperture is given by $\hat{y}E_y$, a magnetic source is formed according to the field equivalence principle. When the width of aperture is sufficiently small, the azimuthal component of electric field
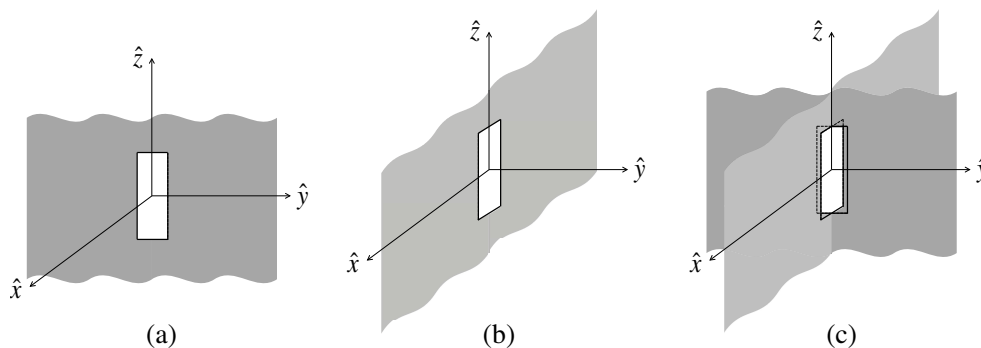
Figure 1. Rectangular aperture on infinite ground plane at different position. (a) On the y-z plane, (b) on the x-z plane, (c) on both y-z plane and x-z plane.

will satisfy the given condition

$$E_\phi^{(a)} \propto E_y \cos\phi \qquad (1)$$

where ϕ is the azimuth angle. The above expression is intuitive since $E_\phi(\phi = 90°)$ and $E_\phi(\phi = 270°)$ are both orthogonal to y-axis, resulting a null at broadside along the ground plane direction.

Next the structure is axially rotated 90 degree around the z-axis, as shown in Fig. 1(b), and the infinite ground is on the x-z plane. The field over the aperture is given by $\hat{x}E_x$, and in this case, the condition that E_ϕ must satisfy becomes

$$E_\phi^{(b)} \propto E_x \sin\phi \qquad (2)$$

Specifically, if we combine the two geometry as shown in Fig. 1(c), making the set of two slots aligned at right angles to each other, and let $E_x = \pm jE_y$, the total electric field is obtained through mathematical superposition

$$E_\phi^{total} \propto E_y e^{\pm j\phi} \qquad (3)$$

This indicates that an omnidirectional pattern can be synthesized using two orthogonal slot dipoles when the field components over the apertures are of equal magnitude and in phase quadrature. The concept of feeding was first presented by Brown in 1935 [17], and multiple copies of the crossed dipole pair were arranged to generate a horizontally polarized wave.

It is interesting to note that the proposed structure is similar to an ideal magnetic dipole because they are both omnidirectional antennas with horizontal polarization. However, they have different properties for far-field phase distribution. According to (3), the phase varies linearly along the azimuthal angle for the quadrature-fed turnstile slot dipole, but it is a constant for the magnetic dipole.

3. ANTENNA DESIGN

Figure 2(a) depicts the planar configuration of the proposed turnstile slot antenna. The main arm, located at the center of the antenna, has the width of W and length of $2L$. It is designed at 2.6 GHz, and L corresponds to approximately a quarter-wavelength at the operation frequency. The lateral CPW feed will generate the x-oriented electric field, stimulating the equivalent magnetic dipole at z-direction. From the 3D view of Fig. 2(b), it consists of two CPW-fed slot dipoles, which are properly arranged in a perpendicularly conjugate form. Both slots are off-center fed to prevent immediate contact between the feed lines. Coaxial SMA connectors directly connect the CPW feeding lines, and two external coaxial cables will be attached at the end of SMA. Note that the coaxial cables are not shown in this figure. The proposed antenna possesses similar design concepts to the single feed bifilar helix antenna (SFBHA), which was presented first by Amin's group in 2007. A simple rectangular loop antenna is twisted in a specific turn angle to produce an omnidirectional pattern for slant 45° linear polarization [18] or circular polarization [19, 20]. On the other hand, two orthogonal loops (a general form of slot) are employed in this turnstile slot antenna.
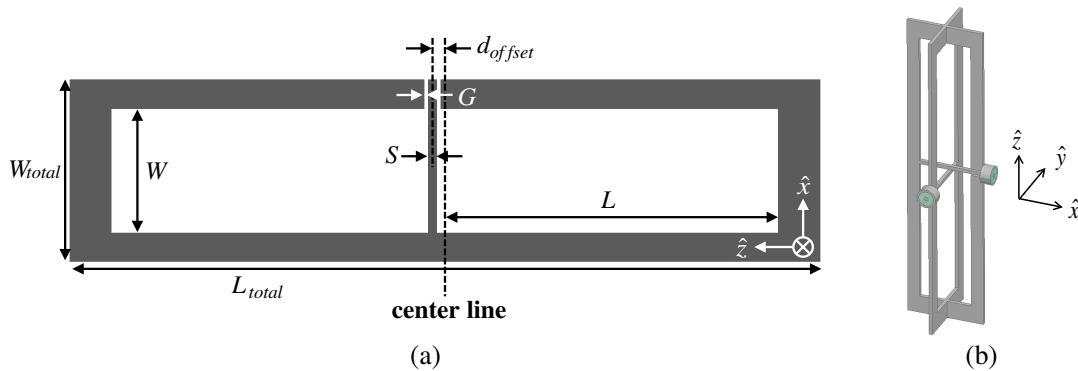
Figure 2. Geometry and dimensions of the proposed antenna. (a) 2D view, (b) 3D view.

To obtain an omnidirectional radiation pattern, the conjugate slot dipoles are fed in equal magnitude with phase quadrature. There are two feasible methods that provide quadrature feed, as shown in Fig. 3. One of them splits the input RF signal equally using a power divider, and then delay one path by an additional 90 degree. Another approach is to employ a branch-line coupler, because the signals at two output ports are intrinsically 90 degree out-of-phase.

(a)   (b)
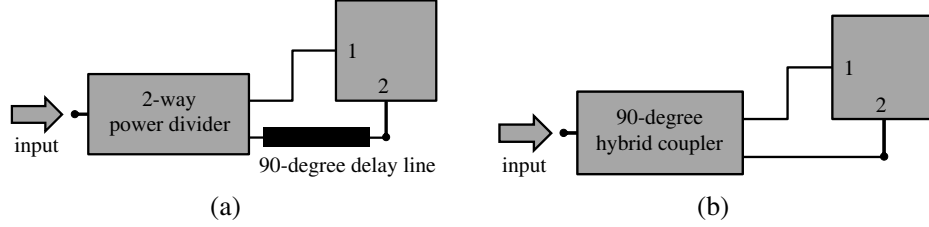
Figure 3. Feeding network of the proposed turnstile slot antenna system. (a) Power divider and delay line, (b) branch-line coupler.

4. SIMULATED AND MEASURED RESULTS

A prototype of the proposed antenna is fabricated and tested. The widths of the strip and gap of the CPW feed line, denoted by S and G, are determined to be 1.0 and 0.5 mm, respectively. The parameters of the turnstile slot dipole are: $W_{total} = 22$ mm, $L_{total} = 90$ mm, $d_{offset} = 1.5$ mm, $W = 15$ mm and $L = 40$ mm. Stainless steel with a thickness $t = 1$ mm is chosen as the material for antenna fabrication. In order to solder the two pieces of slot dipole and SMA connectors, we electroplate nickel on the surface of stainless steel with a thickness of 3 μm.

Figure 4 shows the simulated and measured scattering parameters of the antenna, and reasonable agreement between them can be observed. Due to its symmetric property, only $|S_{11}|$ and $|S_{21}|$ are depicted. The simulation was carried out using the commercial finite element method solver HFSS (high frequency structural simulator). With reference to the simulated result, the antenna is resonant at 2.6 GHz and the impedance bandwidth ($|S_{11}| < -10$ dB) is 8.4% (2.52–2.74 GHz). It can be seen that another resonant mode is found at 1.55 GHz in simulation, which is due to direct coupling between port 1 and port 2 of the antenna. The energy is mainly confined to this structure and does not radiate to the far field. However, the coupling effect is weaker in the experimental result, because the lossy metals: stainless steel and nickel, which were not considered in the simulation phase, consume the power
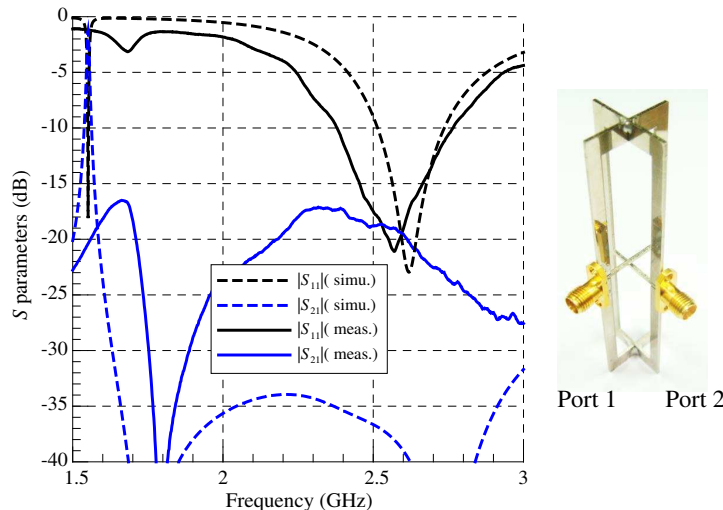
Figure 4. Simulated and measured S-parameters of the turnstile slot dipole antenna with two ports.

in this resonant mode. To investigate how material affects the scattering parameters of the proposed antenna, different types of metal: PEC, stainless steel, and nickel are used for simulation. Notably, the resonant mode for radiation at 2.6 GHz is almost unaffected, but the material has obvious impact on the coupling mode as shown in the inset of Fig. 5, which explains the discrepancy of Fig. 4. Besides, the measured isolation ($|S_{21}|$ and $|S_{12}|$) between port 1 and port 2 is relatively poor. It is due to the
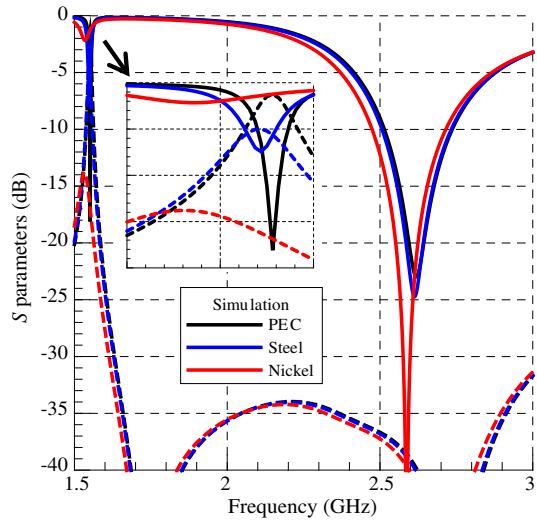
Figure 5. Simulated S-parameters of the turnstile slot dipole antenna using different materials: PEC, stainless steel, and nickel. Solid line represents the $|S_{11}|$ while dotted line the $|S_{21}|$, respectively.
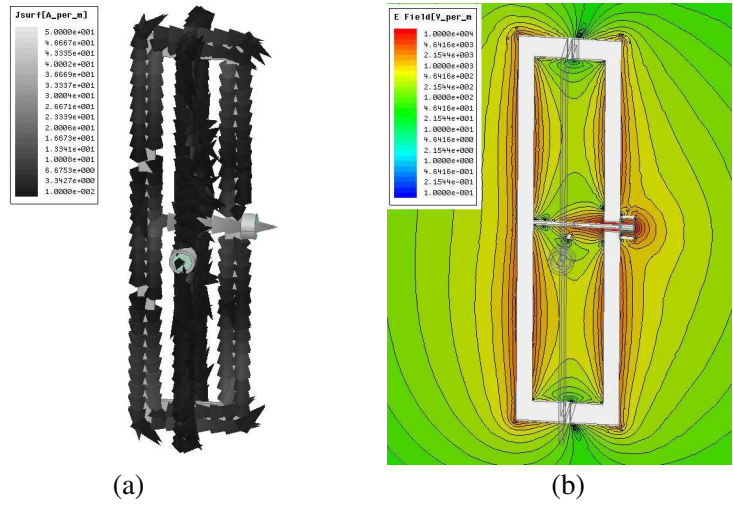
Figure 6. Field distributions of the turnstile slot antenna when port 2 (at the right-hand side) is excited at 2.6 GHz. (a) Vector of surface current, (b) magnitude of electric field.
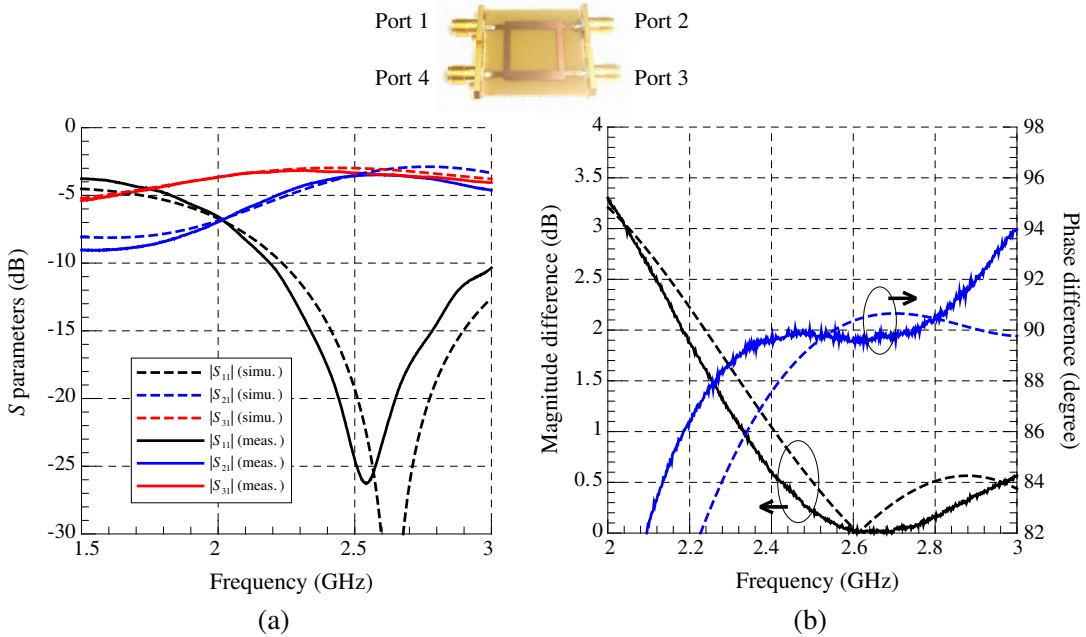
Figure 7. Simulated and measured results of the one-stage branch-line coupler. Dotted lines represent simulation data while solid lines represent measurement data. (a) S-parameters, (b) differences of magnitude and phase for port 2 and port 3.

fabrication tolerance that the two slot dipoles may not be aligned at exact right angles, and the surface roughness should also be taken into account. The field distributions, including the surface current and electric field, at 2.6 GHz are plotted in Fig. 6. Since the ground plane of the proposed slot antenna is so small that the slot is very close to the outer ground edge, the current vectors on the inner and outer edges are approximately the same in magnitude. This will slightly affect the beamwidth of each slot dipole, but the cross-polarization ratio is independent of the ground plane size.

Two possible feeding networks were mentioned in the previous section, and the branch-line coupler is more favorable in practical application since it occupies less area, which is advantageous in volume-limited systems. In this study, a one-stage branch-line coupler designed at 2.6 GHz is employed. Fig. 7(a) demonstrates the reflection and transmission coefficients by exciting port 1 while the isolation port (port 4) is terminated. Meanwhile, the difference between magnitude and phase at port 2 and port 3 are shown in Fig. 7(b). The bandwidth of branch-line coupler is defined by $||S_{21}| - |S_{31}|| < 1\,\text{dB}$ and $|\angle S_{21} - \angle S_{31} - 90°| < 2°$. This criterion can ensure the smoothness of the synthesized omnidirectional pattern.
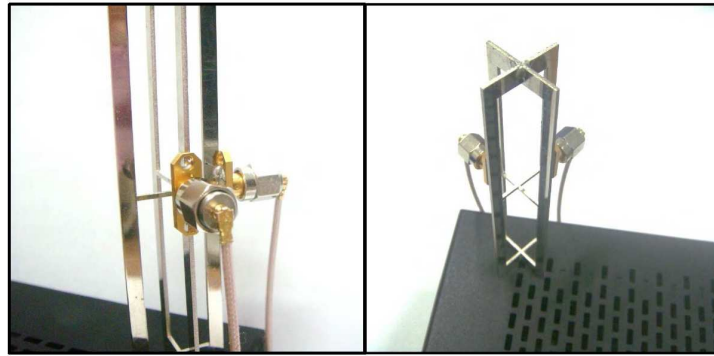
Figure 8. Fabricated turnstile slot antenna connecting two RG-178 cables and a branch-line coupler which is hidden by the housing.

Case 1
(original)

Case 2

Case 3

Case 4

Perspective

(a)
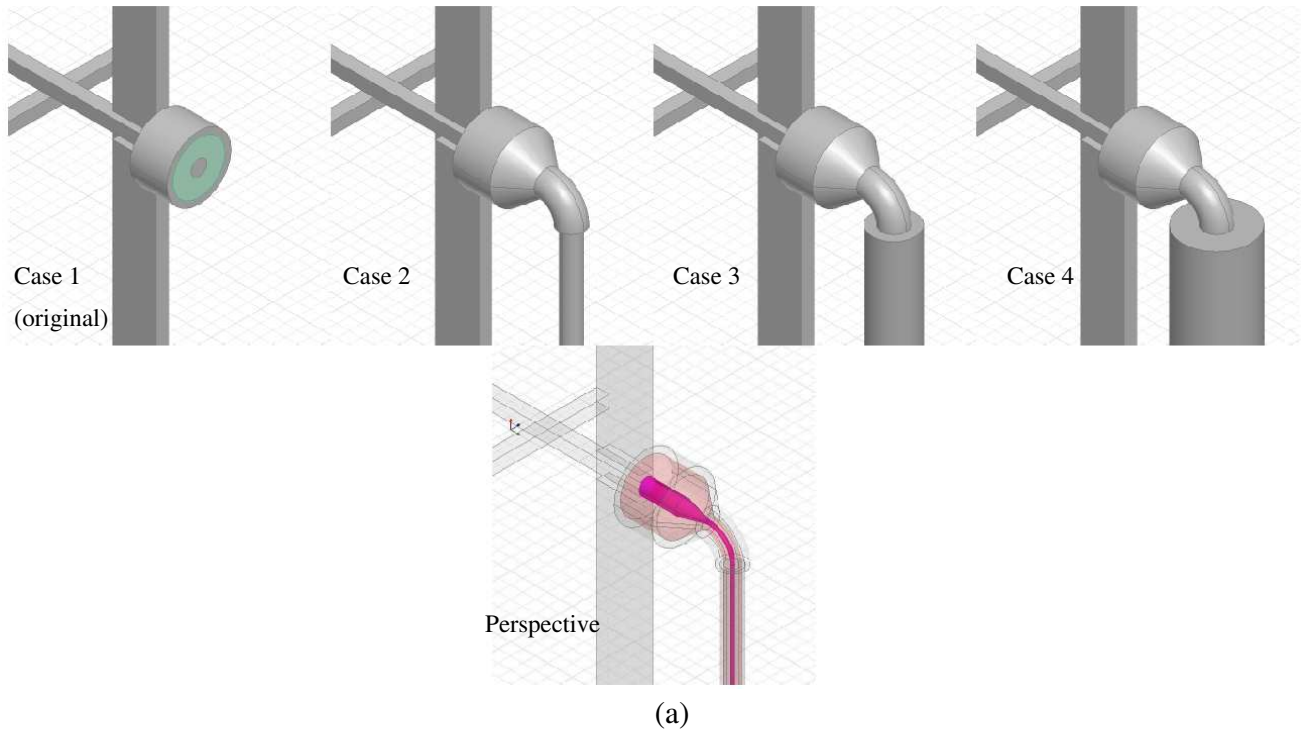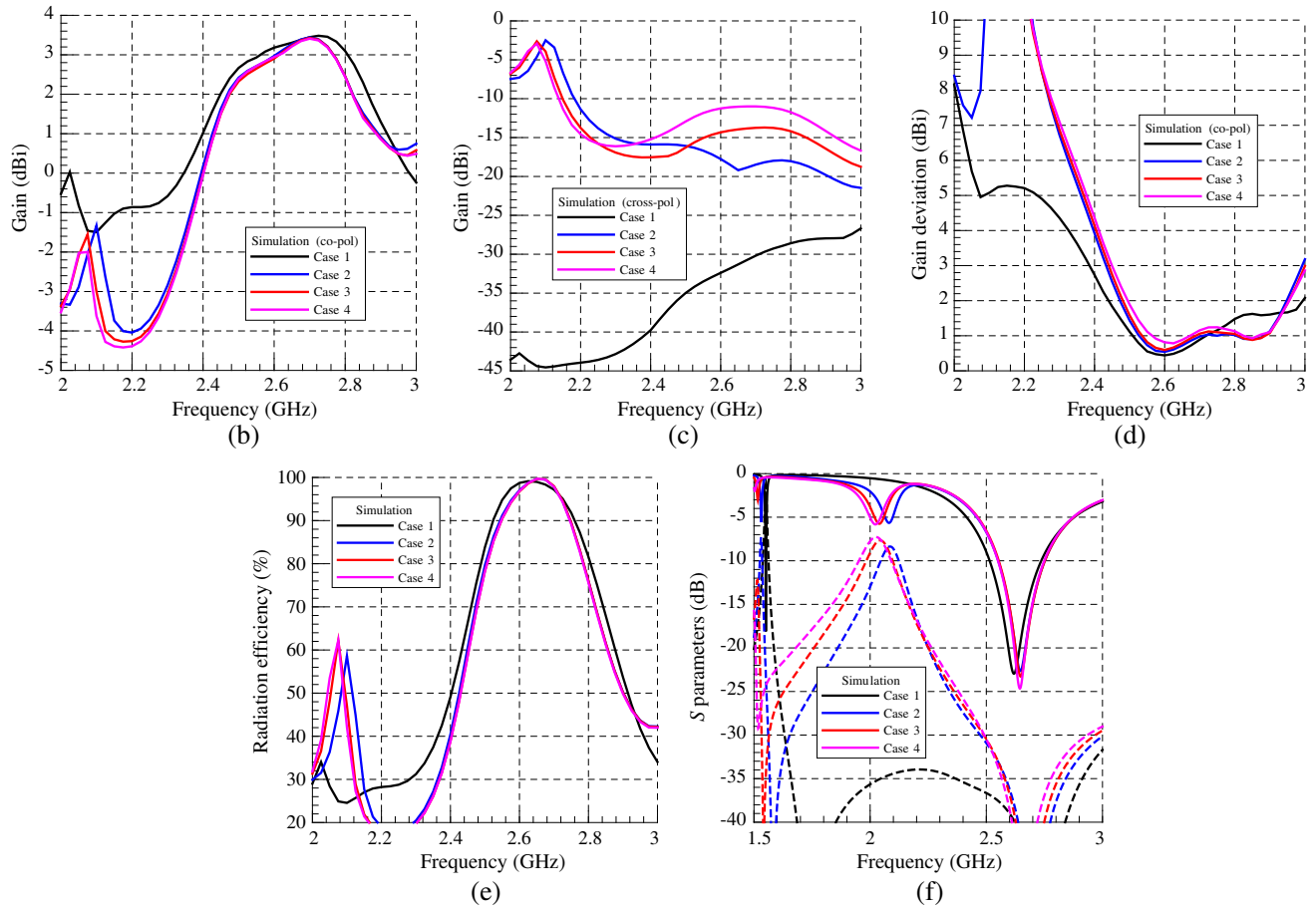
Figure 9. Several antenna characteristics regarding the effect of feeding coaxial line. (a) Geometry of the feeding structure in simulation domain, (b) maximum gain (co-pol at E-plane), (c) maximum gain (cross-pol at E-plane), (d) gain deviation (co-pol at E-plane), (e) radiation efficiency, (f) S-parameters (solid line: $|S_{11}|$, dotted line: $|S_{21}|$).

To verify the principle of the omnidirectional horizontally polarized antenna, we use two thin coaxial cables, both measuring 100 mm, to connect the antenna and coupler. Fig. 8 shows the photo of the entire system, and the RG-178 coaxial cables with IPEX connectors are selected. There is only one branch-line coupler ($30 \times 30 \, \text{mm}^2$) under the plastic housing, and its influence is negligible. However, the radiation pattern will be affected remarkably when a large ground plane is placed in the vicinity. We have studied the influence of the feeding coaxial lines numerically using the topology shown in Fig. 3(b). This is accomplished by the co-simulation of HFSS and Designer, and the results are shown in Fig. 9. Four feeding structures are considered in the simulation. Case 1 is the original structure utilized to obtain the results in Figs. 4–5, while case 2, 3, and 4 illustrate an additional transition from SMA to RG-178 and a coaxial line with different ground thickness. The perspective view of the transition is shown in Fig. 9(a). Simulation results reveal that the maximum gain (G_{max} in the azimuth plane) of co-pol, the gain deviation (defined as the $G_{\text{max}} - G_{\text{min}}$ in the azimuth plane) of co-pol, and the radiation efficiency are scarcely affected from 2.4 to 2.8 GHz. However, the cross-pol component in the azimuth plane increases when the coaxial line becomes thicker, which also explains the thin cable RG-178 is a good choice for the experiment. Particularly, the cable gives rise to another coupling mode at around 2 GHz, but this phenomenon does not appear in the measurement data by virtue of the lossy metals adopted in this paper (stainless steel and nickel). From this parametric study, we can conclude that the influence of outer coaxial cable on radiation characteristics can be reduced if it has small width comparing to the antenna.
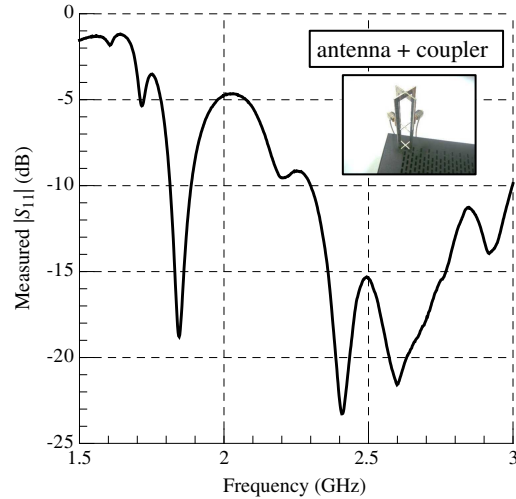
Figure 10. Measured reflection coefficient of the entire system including antenna, coupler, and two coaxial cables.
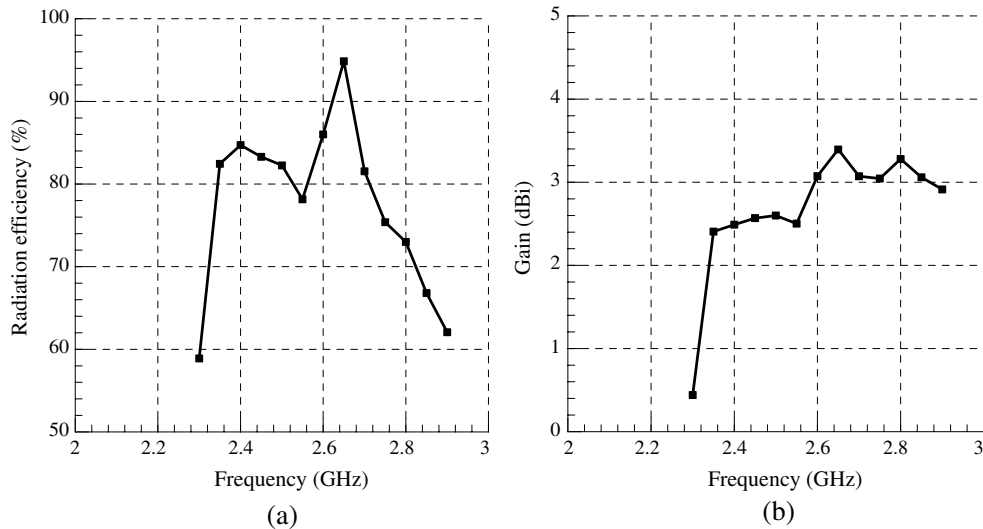
Figure 11. (a) Measured antenna efficiency and (b) gain of the entire omnidirectional antenna system.

The reflection coefficient of the whole structure is shown in Fig. 10. Yet it is not suitable to evaluate the antenna performance entirely through this figure, because the input power will also be consumed by the $50\,\Omega$ terminator located on the branch-line coupler. Consulting the radiation efficiency will be a preferable choice. We tested the antenna in a spherical near-field anechoic chamber. The radiation characteristics of the antenna are obtained by the near-field measurement in combination with a near-field far-field transformation (NFFFT). The radiated efficiency is defined as the power radiated through the antenna to the power fed to the antenna terminal. Fig. 11(a) shows the measured total antenna efficiency that has taken both the impedance matching and termination into account. The bandwidth of the antenna is defined with radiation efficiency larger than 70%.

Moreover, the usable bandwidth that provides both omnidirectional pattern and reasonable radiated power is the overlapping region of the bandwidth of branch-line coupler and antenna. The measured usable bandwidth is 15.4% (2.4–2.8 GHz), and the maximum measured gain across the region is given by 2.5 dBi, as shown in Fig. 11(b). The measured total efficiency of the antenna varies between 73% and 95% within the operating band. Figs. 12 and 13 depict the measured radiation patterns at x-y plane (E-plane) and y-z plane (H-plane), respectively. The measurement is taken from 2.4 to 2.8 GHz with a step of 0.05 GHz. It is clear that smooth omnidirectional radiation patterns with horizontal
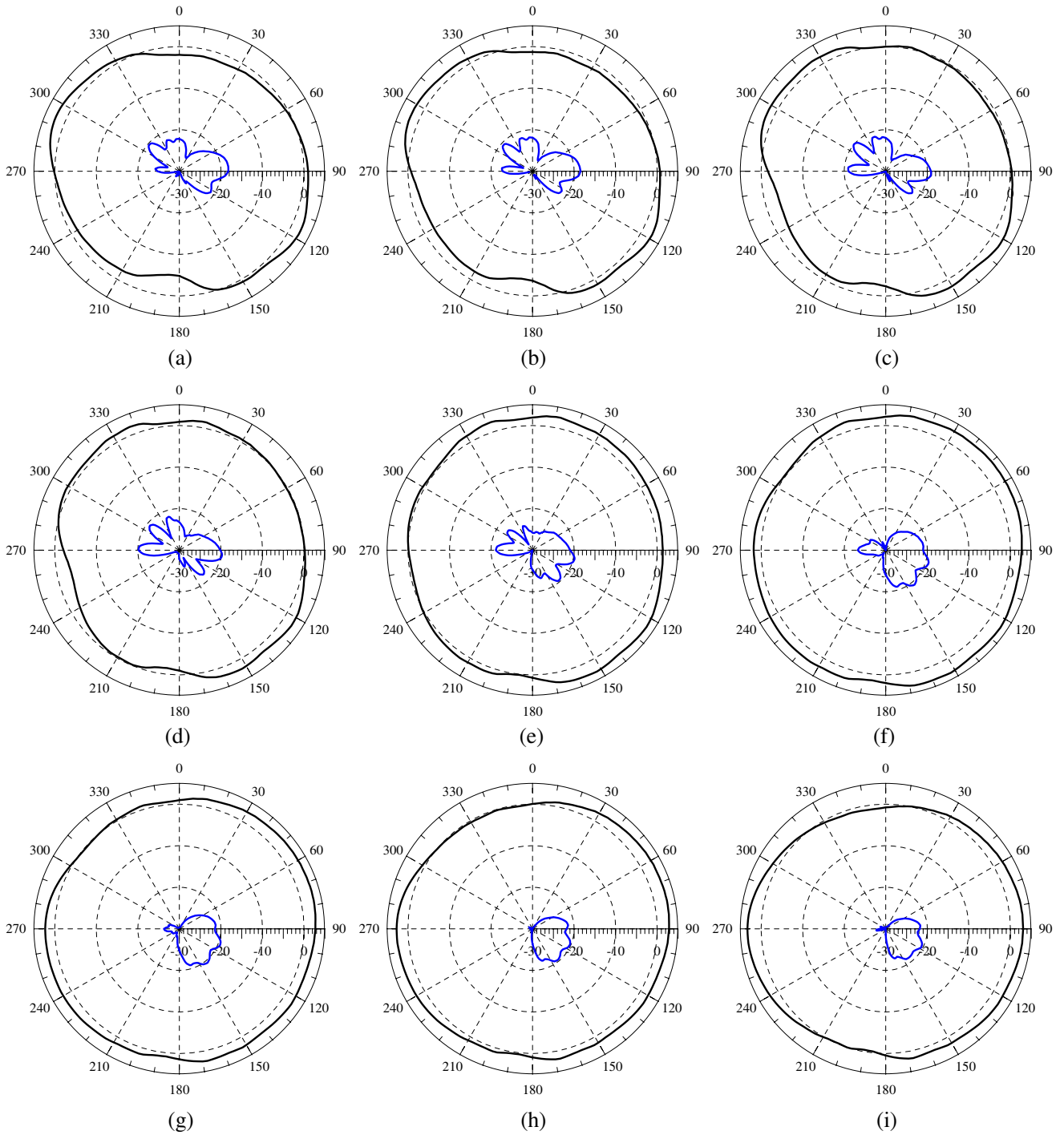
Figure 12. Measured radiation patterns for the HP omnidirectional antenna at x-y plane (E-plane). The black curve represents co-polarization and the blue curve represents cross-polarization. (a) 2.40 GHz, (b) 2.45 GHz, (c) 2.50 GHz, (d) 2.55 GHz, (e) 2.60 GHz, (f) 2.65 GHz, (g) 2.70 GHz, (h) 2.75 GHz, (i) 2.80 GHz.

polarization in the azimuth plane are obtained, and some pattern distortion occurs at $\phi = 180°$ and $\phi = 270°$ because of the surrounding SMA connectors and coaxial cables (shown in Fig. 8). The co-pol component is stronger than cross-pol counterpart by about 20 dB, which shows that this system has good polarization purity.
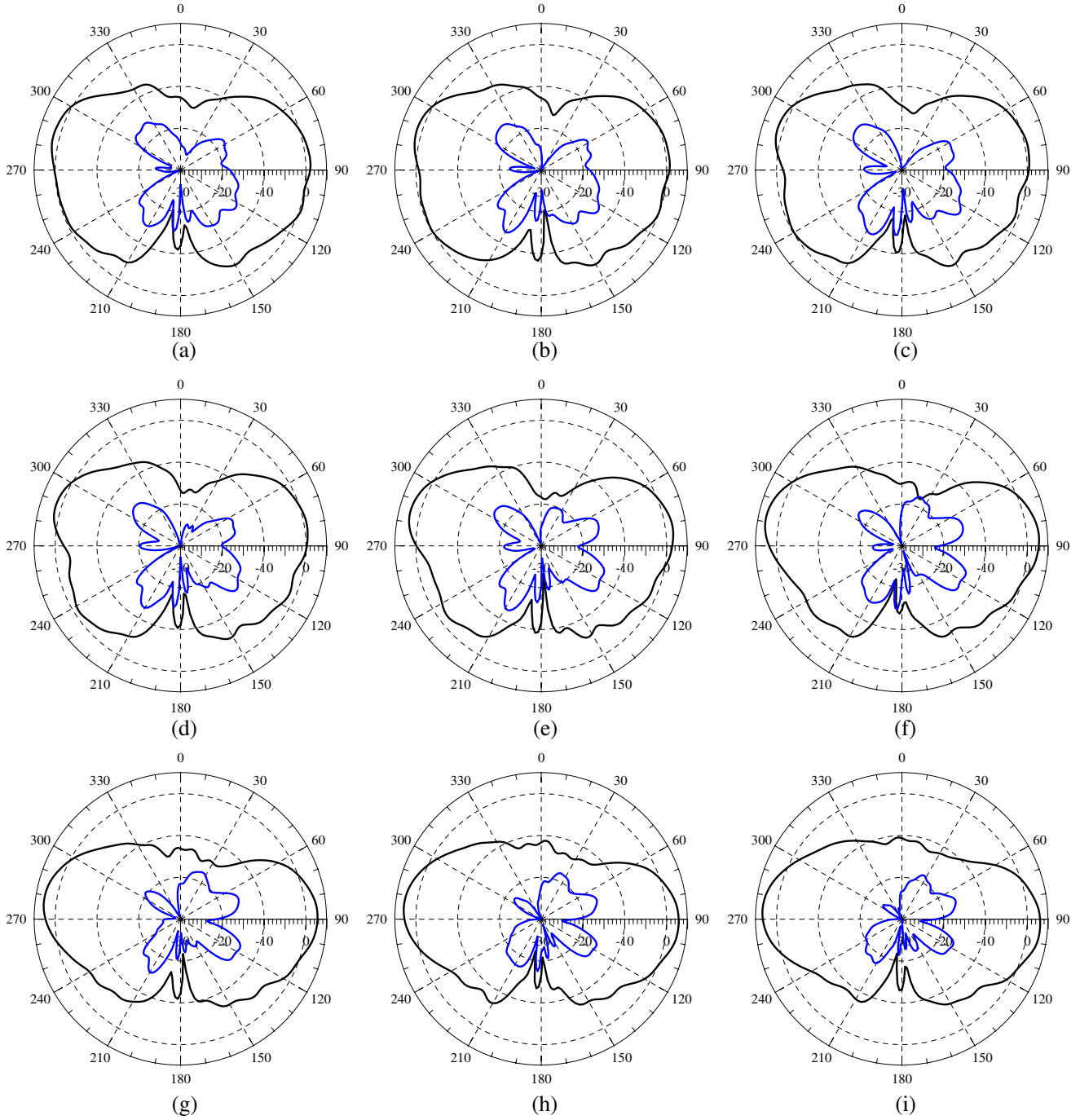
Figure 13. Measured radiation patterns for the HP omnidirectional antenna at y-z plane (H-plane). The black curve represents co-polarization and the blue curve represents cross-polarization. (a) 2.40 GHz, (b) 2.45 GHz, (c) 2.50 GHz, (d) 2.55 GHz, (e) 2.60 GHz, (f) 2.65 GHz, (g) 2.70 GHz, (h) 2.75 GHz, (i) 2.80 GHz.

5. CONCLUSION

A turnstile slot dipole is proposed in this paper. It is constructed by intersecting two slot dipoles perpendicularly and thus maintaining the property of horizontal polarization. This antenna exhibits omnidirectional radiation pattern when fed by two signals of equal amplitude with phase quadrature. A prototype that operates from 2.4 to 2.8 GHz is fabricated and investigated. The system yields a peak

gain in the range of 2.5–3.4 dBi through the entire operational bandwidth with the radiation efficiency greater than 73%. The appearance of the turnstile slot dipole is tall and thin rather than the regular planar shape, which is suitable to be disguised as poles or masts for indoor or base station applications. Moreover, it can also be employed as one of a pair of orthogonally polarized MIMO antenna system.

REFERENCES

1. Vaughan, R. G., "Polarization diversity in mobile communications," *IEEE Trans. Veh. Technol.*, Vol. 39, No. 3, 177–186, 1990.

2. Balanis, C. A., *Antenna Theory: Analysis and Design*, John Wiley & Sons, 2012.

3. Alford, A. and A. G. Kandoian, "Ultrahigh-frequency loop antennas," *Trans. AIEE*, Vol. 59, No. 12, 843–848, 1940.

4. Lin, C.-C., L.-C. Kuo, and H.-R. Chuang, "A horizontally polarized omnidirectional printed antenna for WLAN applications," *IEEE Trans. Antennas Propag.*, Vol. 54, No. 11, 3551–3556, 2006.

5. Ahn, C.-H., S.-W. Oh, and K. Chang, "A dual-frequency omnidirectional antenna for polarization diversity of mimo and wireless communication applications," *IEEE Antennas Wireless Propag. Lett.*, Vol. 8, 966–969, 2009.

6. Wu, B. Q. and K.-M. Luk, "A wideband low-profile conical beam antenna with horizontal polarization," *Asia Pacific Microwave Conference*, 1806–1808, 2009.

7. Zhang, G., H. Zhang, Z. Yuan, Z. Wang, and D. Wang, "A novel broadband *E*-plane omni-directional planar antenna," *Journal of Electromagnetic Waves and Applications*, Vol. 24, Nos. 5–6, 663–670, 2010.

8. Quan, X. L., R. L. Li, J. Y. Wang, and Y. H. Cui, "Development of a broadband horizontally polarized omnidirectional planar antenna and its array for base stations," *Progress In Electromagnetics Research*, Vol. 128, 441–456, 2012.

9. Wei, K., Z. Zhang, and Z. Feng, "Design of a wideband horizontally polarized omnidirectional printed loop antenna," *IEEE Antennas Wireless Propag. Lett.*, Vol. 11, 49–52, 2012.

10. Yu, Y., F. Jolani, and Z. Chen, "A wideband omnidirectional horizontally polarized antenna for 4G LTE applications," *IEEE Antennas Wireless Propag. Lett.*, Vol. 12, 686–689, 2013.

11. Kawakami, H., G. Sato, and R. Masters, "Characteristics of TV transmitting batwing antennas," *IEEE Trans. Antennas Propag.*, Vol. 32, No. 12, 1318–1326, 1984.

12. Radnovic, I., A. Nesic, and B. Milovanovic, "A new type of turnstile antenna," *IEEE Antennas Propag. Mag.*, Vol. 52, No. 5, 168–171, 2010.

13. Ando, A., K. Cho, and T. Hori, "Dielectric-loaded slotted-cylinder antennas offering reduced base station interference for personal communication services," *Antennas and Propagation Society International Symposium*, Vol. 3, 1454–1457, 1998.

14. Ando, A., A. Kondo, and S. Kubota, "A study of radio zone length of dual-polarized omnidirectional antennas mounted on rooftop for personal handy-phone system," *IEEE Trans. Veh. Technol.*, Vol. 57, No. 1, 2–10, 2008.

15. Li, Y., Z. Zhang, J. Zheng, and Z. Feng, "Compact azimuthal omnidirectional dual-polarized antenna using highly isolated colocated slots," *IEEE Trans. Antennas Propag.*, Vol. 60, No. 9, 4037–4045, 2012.

16. Fenn, A., "Arrays of horizontally polarized loop-fed slotted cylinder antennas," *IEEE Trans. Antennas Propag.*, Vol. 33, No. 4, 375–382, 1985.

17. Brown, G. H., "Antenna system," U. S. Patent 2,432,858, Dec. 1947.

18. Amin, M., R. Cahill, and V. Fusco, "Single feed low profile omnidirectional antenna with slant 45° linear polarization," *IEEE Trans. Antennas Propag.*, Vol. 55, 3087–3090, 2007.

19. Amin, M., J. Yousaf, and S. Iqbal, "Single feed circularly polarised omnidirectional bifilar helix antennas with wide axial ratio beamwidth," *IET Microw. Antennas Propag.*, Vol. 7, 825–830, 2013.

20. Yousaf, J., M. Amin, and S. Iqbal, "Design of circularly polarized omnidirectional bifilar helix antennas with optimum wide axial ratio beamwidth," *Progress In Electromagnetics Research C*, Vol. 39, 119–132, 2013.